Multi-Channel Phase-Sensitive Amplification in a Low Loss CMOS-Compatible Spiral Waveguide

YANBING ZHANG, [1,*] CHRISTIAN REIMER, [1] JENNY WU, [1] PIOTR ROZTOCKI, [1] BENJAMIN WETZEL, [1,2] BRENT E. LITTLE, [3] SAI T. CHU, [4] DAVID J. MOSS, [5] BENJAMIN J. EGGLETON, [6] MICHAEL KUES, [1,7] AND ROBERTO MORANDOTTI [1,8,9*]

[1]*INRS-EMT, 1650 Boulevard Lionel-Boulet, Varennes, Québec J3X 1S2, Canada*
[2]*School of Mathematical and Physical Sciences, University of Sussex, Falmer, Brighton BN1 9RH, UK*
[3]*State Key Laboratory of Transient Optics and Photonics, Chinese Academy of Science, Xi'an, China*
[4]*City University of Hong Kong, Department of Physics and Material Science, Tat Chee Avenue, Hong Kong, China*
[5]*Center for Micro-Photonics, Swinburne University of Technology, Hawthorne, Victoria 3122, Australia*
[6]*CUDOS,IPOS, School of Physics, University of Sydney, Sydney, NSW 2006, Australia*
[7]*School of Engineering, University of Glasgow, Rankine Building, Oakfield Avenue, Glasgow G12 8LT, UK*
[8]*Institute of Fundamental and Frontier Sciences, University of Electronic Science and Technology of China, Chengdu 610054, China*
[9]*National Research University of Information Technologies, Mechanics and Optics, St Petersburg, Russia*
**Corresponding author: yanbing.zhang@emt.inrs.ca, morandotti@emt.inrs.ca*

Received XX Month XXXX; revised XX Month, XXXX; accepted XX Month XXXX; posted XX Month XXXX (Doc. ID XXXXX); published XX Month XXXX

We investigate single-channel and multichannel phase-sensitive amplification (PSA) in a highly nonlinear, CMOS-compatible spiral waveguide with ultralow linear and negligible nonlinear losses. We achieve a net gain of 10.4 dB and an extinction ratio of 24.6 dB for single channel operation, as well as 5dB gain and 15 dB extinction ratio spanning over a bandwidth of 24 nm for multiple channel operation. In addition, we derive a simple analytic solution that enables the calculation of the maximum phase-sensitive gain in any Kerr medium featured by linear and nonlinear losses. These results not only give a clear guideline for designing PSA-based amplifiers, but also show that it is possible to implement both optical regeneration and amplification in a single on-chip device.

OCIS codes: (190.4410) Nonlinear optics, parametric processes; (190.4380) Nonlinear optics, four-wave mixing; (190.3270) Kerr effect.

Nonlinear optical parametric processes have been used in a wide variety of fields ranging from optical signal processing [1, 2] and frequency comb sources [3] to quantum photonics [4, 5]. In particular, phase-sensitive amplification (PSA), a parametric scheme exploiting phase-dependent optical gain, has shown great promise in both classical and non-classical optical applications. Specifically, in fiber-optic communications, PSA-based regenerators have been applied to higher-order modulation formats [1], and PSA-based amplifiers have demonstrated the capability to overcome the 3 dB quantum noise limit imposed by stimulated-emission-based amplifiers such as Raman and erbium-doped fiber amplifiers (EDFAs) [2]. In quantum optics, PSA has been used to generate squeezed states of light [4] and to noiselessly amplify entangled photon sources [5]. So far, PSA applications have mainly been based on optical fibers or temperature-controlled $\chi^{(2)}$-PPLN waveguides. In order to exploit these effects in scalable and compact implementations, on-chip $\chi^{(3)}$ PSA has recently been realized in various platforms since the first demonstration on chalcogenides [6, 7], such as crystalline [8, 9] and amorphous [10] Si, GaInP [11], AlGaAs [12], as well as SiGe [13]. However, in these material systems, either the platform lacks of compatibility with CMOS fabrication processes [6, 7, 11, 12] or the important parameters of the PSA, such as the net gain or extinction ratio (ER), are limited due to high linear [10] and nonlinear [8] losses, unless PIN junctions are employed at the cost of increased device complexity [9]. Therefore, a stable CMOS-compatible nonlinear platform with low loss is highly desirable for PSA applications. In parallel to these developments in materials and optical integration, novel schemes have been devised to increase information processing capabilities, among them multiple-frequency operation over broad optical bandwidths. However, only a few woks on PSA report the simultaneous processing of two or more channels in a single device, e.g. PPLN waveguides [1] and optical fibers [14, 15], while all investigations of on-chip $\chi^{(3)}$ PSA have been restricted to a single channel [6-13]. Indeed, thus far, the investigation of multi-channel PSA has not been carried out in an integrated $\chi^{(3)}$ medium.

In this work, we experimentally investigate single- and multi-channel one-pump PSA processes in a CMOS-compatible, high-refractive-index glass waveguide made from Hydex glass [16]. The ultra-low propagation loss (0.08 dB cm^{-1}), moderate nonlinearity ($\gamma = 0.22$ W^{-1}m^{-1}), and negligible nonlinear loss in the C-band

enable a large net gain of 10.4 dB and a significant ER of 24.6 dB for single channel PSA in a 45 cm-long spiral waveguide. Additionally, we demonstrate four-frequency-channel PSA with an ER of 15 dB and a net gain of 5 dB, with tunable operation achieved by controlling the initial phases of the individual channels. Finally, we derive a simple analytic formula capable of predicting the net gain in any $\chi^{(3)}$ media in the presence of linear and nonlinear losses.

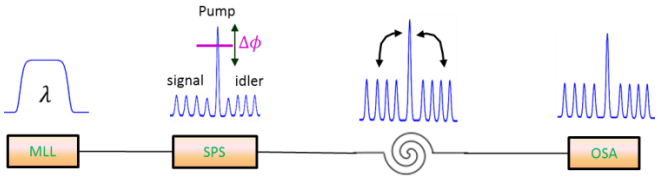

Fig. 1. Experimental setup. The strong pump and weak signal/idler pairs were sliced by a spectral pulse shaper (SPS) from a broadband mode-locked laser (MLL) pulse with a 16.8 MHz repetition rate. The SPS was also used to control the power and phase change of each mode, e.g. $\Delta\phi$, in the pump phase. The TE polarization is guided into a pigtailed Hydex waveguide (45-cm long), where the PSA process occurs. The phase-dependent output spectrum was recorded by an optical spectral analyzer (OSA). The blue traces are schematics of the spectral intensity profiles at each stage.

The high-intensity pump and phase-locked low-intensity signal/idler fields were generated by using a spectral pulse shaper to spectrally tailor a broadband input pulse from a mode-locked laser (Fig. 1). In order to achieve sufficient optical power, we also used an EDFA after spectral tailoring of the initial pulse (not shown in Fig. 1). To eliminate any PSA in the EDFA, we implemented a temporal delay between the pump and signal/idler waves [6-8], which was reversed before injecting it into the chip. Using a polarization controller, the field was then coupled to the TE mode of our pigtailed waveguide, where the PSA occurred through the degenerate four-wave mixing (FWM) process [7]. This process was then characterized by changing the relative spectral phases between the different channels, e.g. via changing the phase of the pump field (e.g. $\Delta\phi$ in Fig.1) and/or the weak fields. The output spectra were recorded by means of an optical spectral analyzer. The total loss of the waveguide was 7 dB, including the coupling loss of 1.75 dB/facet and a total propagation loss of 3.5 dB over the 45 cm length of the spiral waveguide.

We first investigated single-channel PSA gain with one pair of signal and idler fields. The input signal/pump/idler pulses with a temporal width of 8 ps were centered at 1551 nm, 1555 nm, and 1559 nm, respectively. The peak power of the signal/idler was $P_{s,i} = 0.14$ W. In order to show that the gain experienced by the weak fields is phase-dependent, we changed the pump phase with a detuning step of 0.1 rad over the range $[0, \pi]$ (equivalent to one period) while keeping the signal and idler phases constant. We characterized the on-chip gain (G) of the weak waves as the ratio between their output and input intensities [7]. As the gain curves for the signal and idler were identical within the measurement uncertainty, only the signal gain was considered (Fig. 2(a)). We obtained a maximum gain (G_{max}) of 9.8 dB at $\Delta\phi = 0.10\pi$ and a minimum gain (G_{min}) of -14 dB at $\Delta\phi = 0.61\pi$ for an input peak pump power of 42 W. This corresponds to an ER of $G_{max} - G_{min}$ = 23.8 dB. Similar to other on-chip platforms [6-13], the unitary PSA relationship of $G_{max} \times G_{min} = 1$ does not hold for our high nonlinear material platform due to the propagation loss [7].

Our experimental observations showed excellent agreement with the numerical calculations obtained by solving the nonlinear Schrödinger equation (NLSE) using the split-step Fourier method [7], see inset in Fig. 2(a). In our calculations, the waveguide dispersion at the pump wavelength is estimated up to the fourth order, see [16] for explicit values. Note that although the input signal/idler powers are set to 23 dB lower than the pump, in order to minimize cascaded FWM among the input channels, the contribution of cascaded FWM is still clearly observable in the output spectrum.

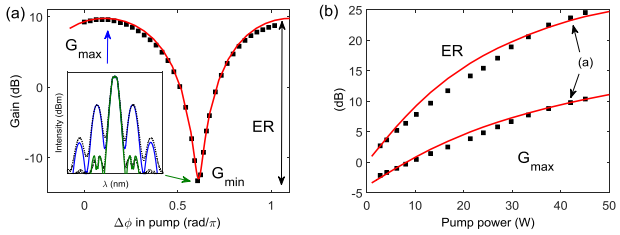

Fig. 2. (a) Experimental (squares) and numerically calculated (solid line) phase-sensitive gain of the signal wave at a peak pump power of 42 W, as a function of the pump phase detuning ($\Delta\phi$) with a periodicity of π. Inset: Simulated results (blue and green) agreed with the measured output spectra at the maximum (G_{max}) and minimum (G_{min}) gain, respectively. (b) Both the maximum gain and extinction ratio (ER) increase with the pump power without reaching saturation.

Next, we investigated the effect of the pump power on the PSA gain. In particular, we repeated the process of Fig. 2(a) at each pump power and characterized the power-dependence of G_{max} and ER, see Fig. 2(b). At low pump powers, since the signal's gain is dominated by propagation loss in the integrated waveguide, the gain curve converges to -3.5 dB, and thus the ER approaches zero dB. At higher power levels, both G_{max} and ER increase gradually with the pump power. The measured 10.4 dB G_{max} and 24.6 dB ER are comparable to the best values found in the literature, which are 12.5 dB G_{max} obtained in chalcogenides [7] and 28.6 dB ER achieved in SiGe [13], respectively. Remarkably, both of these values do not exhibit a clear saturation at high powers in the Hydex waveguides, in contrast to other platforms, such as silicon, GaInP, and chalcogenide waveguides. This lack of saturation here agrees with the fact that an unsaturated FWM conversion (i.e. phase-insensitive operation) was observed in the same platform with a maximum peak pump power up to 40 W [16]. However, in silicon and GaInP, the nonlinear and (high) linear loss significantly limit the maximum gain to a few dBs [8-11], while in chalcogenide waveguides, the ER saturates due to a reduction in the absolute value of the minimum gain [7].

We then investigated four-frequency-channel PSA in our low-dispersion Hydex waveguides. To cover the required spectrum, we used a different laser with a broader spectral bandwidth. The pulse duration and spectral bandwidth was chosen to be the same for the single- and multi-channel operation, however in the latter case, a larger over-all bandwidth associated to the seeded waves was required. This resulted in an available peak power of 22 W for the pump and of around 10mW for each individual spectral channel. The pump wavelength was fixed at 1550 nm and all the signal/idler channels were symmetrically frequency detuned from the pump with a 440 GHz equidistant channel separation. To achieve multi-channel PSA, we first obtained the relative phase for the minimum gain in each

channel (i.e. without any other channels active), and then compensated the corresponding phase offsets in the weak waves at the spectral pulse shaper. We were able to obtain selective amplification, e.g. the first and third channels experienced losses while the second and the fourth channels were amplified, and vice versa, as shown by the gain curves in Fig. 3(a). This was confirmed by the corresponding output spectra at minimum and maximum amplifications (Fig. 3(b)). Furthermore, the four-channel synchronous amplification shown in Fig. 3(c) was achieved by adding an initial π phase in channel two and four. On average, we achieved a maximum gain of 5 dB (specifically, 6.2/5.3/4.2/4.3 dB at the 1st/2nd/3rd/4th channel, respectively) and an ER of around 15 dB for all the channels in both the selective and synchronous amplification cases. These values are consistent with the results of the one-channel case shown in Fig. 3(a) at a pump power of 22 W. The total bandwidth considering all four-channels was 24 nm, limited by the experimental setup (i.e. the bandwidths of the laser and the spectral pulse shaper). Thanks to the low anomalous dispersion and uniform propagation loss, this PSA operation bandwidth can be extended to 200 nm, as attested by a modulation instability gain over such a large spectral window in the phase-insensitive case [16]. For instance, the calculated temporal walk-off was less than one picosecond and the measured loss variation was < 2 dB over a 200 nm spectral bandwidth.

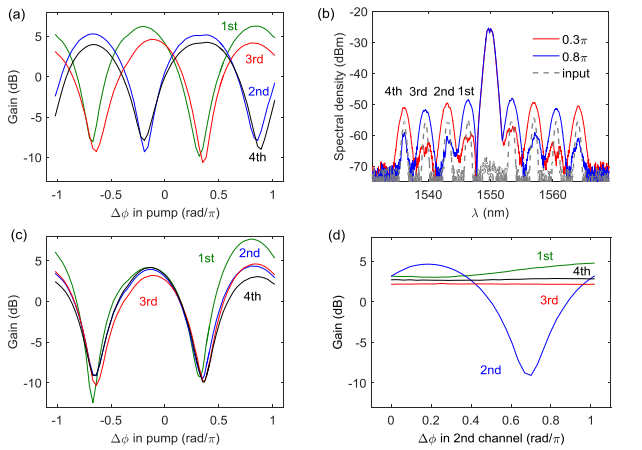

Fig. 3. (a) Selective amplification of individual channels. The 1st and 3rd channels were amplified while the 2nd and 4th channels were attenuated, and vice versa. (b) Input (dashed) and output (solid) spectra for the maximum and minimum gains in (a). (c) Gain curves of the synchronized amplification for the four channels. All the channels reach the maximum and minimum gains at the same phase detuning. (d) Low crosstalk in the four-channel operation. Phase-sensitive gain only occurs in the 2nd channel while the other channels remain nearly constant when a phase detuning is selectively applied in channel 2nd.

We analyzed the crosstalk among the multiple PSA channels by changing the phase in the 2nd channel of one period while leaving the pump phase fixed, when all the channels were synchronized. It was confirmed that only the gain in channel 2 was phase-sensitive, in contrast to that in the other channels, as shown in Fig. 3(d). The small crosstalk (~ 1dB gain variation in 1st channel) was due to multiple-seeded and cascaded FWM processes. These spurious effects are more of a problem in our case as the generated FWM components spectrally overlap with the seeded signal/idler fields. To avoid crosstalk, the spectral locations of the weak waves need to be considered carefully. For example, the frequency separation of the common pump with each signal should be a non-integer multiple of their channel spacing. In addition, this crosstalk effect can be further minimized by reducing the input signal powers. Based on our experiment and numerical simulations, we suggest that the input powers of the signal and idler input fields should be 30 dB lower than the pump power.

In practical PSA-based applications, a large ER is desirable for optical regeneration and generation of squeezing light, while high gain PSA is critical for low-noise amplifiers. Although on-chip PSA with large ER (e.g. >20dB in [9]) has been demonstrated in various platforms, the maximum gains reported are usually only a few dBs (<4 dB in [9]) due to high linear and nonlinear losses. Thus, it is important to assess which mechanism fundamentally limits the net gain in these platforms. A semi-analytic solution of the one-channel PSA process has been derived assuming a slow variation of the pump depletion along the propagation distance [17]. Here, we provide a simple analytic formula to estimate the maximal gain ($G_{\max}$) in any Kerr platform in the presence of linear and nonlinear absorption. In a PSA process, the weak waves simultaneously experience amplification due to the parametric process and attenuation because of the loss. Therefore, assuming that phase-matching is satisfied, $G_{\max}$ is the product of the two processes,

$$G_{\max} = \exp(\phi_{\text{eff}}) = \exp(\gamma P L_{\text{eff}}) \times \exp(\exp(-\alpha_s L)) \quad (1)$$

Here we define the effective phase shift $\phi_{\text{eff}} = \gamma P L_{\text{eff}} e^{-\alpha_s L}$ to consider both the generation and the attenuation experienced by the signal, given by $\exp(\gamma P L_{\text{eff}})$ and $\exp(\exp(-\alpha_s L))$. The effective length is $L_{\text{eff}} = a_p^{-1}(1 - e^{-\alpha_p L})$, while $P = 2P_{\text{in}}$ and $P = P_{1,\text{in}} + P_{2,\text{in}}$ for the one- and two-pump cases. Here P_{in} is the single input pump power. The total losses $\alpha_{s,p}$ on the signal and pump include linear and nonlinear contributions depending on the platform used. Since the derivation and conclusion are similar for materials with TPA, e.g. silicon, and multiple photon absorption, e.g. GaInP [11, 17], here we take only silicon as an example. To fairly compare the material intrinsic properties, we assume that the TPA-induced free-carrier effects can be minimized by using a PIN junction [9]. Since the TPA-induced attenuation α_{TPA} on the signal is twice as strong as on the pump due to cross-phase modulation [18], we obtain $\alpha_p = a + \alpha_{\text{TPA}}$ while $\alpha_s = a + 2\alpha_{\text{TPA}}$, with $\alpha_{\text{TPA}} = L^{-1} \ln(1 + \gamma_{\text{tpa}} P L_0)$, $L_0 = a^{-1}(1 - e^{-aL})$, waveguide length L and effective TPA coefficient γ_{tpa}. Here α_{TPA} is derived from [18] by rewriting Eq. (2) in the form $P_{\text{out}} = P_{\text{in}} e^{-\alpha L} e^{-\alpha_{\text{TPA}} L}$. Therefore, we emphasize that both linear and nonlinear losses have a two-fold contribution in reducing the signal gain, i.e., they not only limit the PSA gain by depleting the pump power during propagation (and thus L_{eff}), but also attenuate the amplified waves. The interaction between generation and attenuation determines the maximum gain. To assess the validity of our approach and simple formula, we summarized the maximum gains in a variety of $\chi^{(3)}$-platforms with different values of linear and nonlinear losses (see Fig. 4(a)). Good agreement was obtained between the experimental gain reported in the literature (squares) and the analytical predictions (solid line) obtained from Eq. (1).

To compare the performance of PSA in different integrated $\chi^{(3)}$-media, we summarized the ERs and maximum gains in Fig. 4. A large $G_{\max}$ should result in a large ER according to its definition. In addition, in the lossless case, the ER is simplified to be twice the maximum gain (dashed line). Although this relation does not hold

for on-chip PSA, we can still clearly observe a trend where the ER generally increases with the maximum gain. Among these media, low-loss Hydex is the only platform which has demonstrated a net gain >10 dB and an ER >20 dB. For materials with a large nonlinearity, both the nonlinear and the (large) propagation loss significantly restrict the maximum gain, although they might not impact the extinction ratio. For example, while the nonlinearities in silicon nanowires [9] and GaInP photonic crystal waveguides [11] are at least one order of magnitude larger than those of chalcogenide and Hydex, their high TPA and large linear loss (30 dB/cm) limit the achievable net gains to 4 dB and 3 dB, respectively. Therefore, although a large community in nonlinear photonics is heavily pushing for new platforms with high nonlinearity [10-13], we may suggest that developing platforms with moderate nonlinearity and low loss is a more efficient way to improve nonlinear performances, particularly for parametric processes involving multiple wave interactions, e.g. PSA.

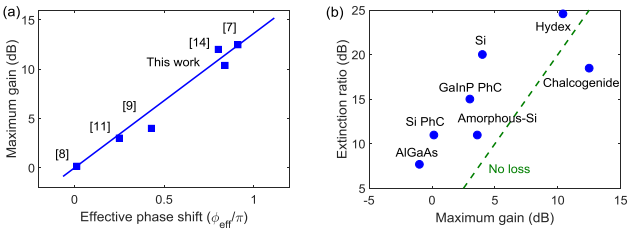

Fig. 4. (a) Our derived analytic formula in Eq.(1) (solid line) is capable of predicting the maximum gains (squares) in various $\chi^{(3)}$-based PSAs with linear and nonlinear loss effects. (b) The extinction ratio (ER) of integrated PSA generally increases with its maximum gain (G_{max}). In the lossless case (dashed line), $ER = \exp(2\gamma PL) = G_{\max}^2$ [7]. PhC is short for photonic crystal. Hydex has been demonstrated to provide both a large gain (>10 dB) and extinction ratio (>20 dB).

We can use Eq. (1) to determine what limits the net gain in materials exhibiting both linear and nonlinear losses. Considering silicon as an illustrative example, a 10 dB gain requires an effective phase shift of $\phi_{\text{eff}} \sim 0.74\,\pi$ according to Fig. 4(a). Using 200 mW input peak power in a 5-cm long typical silicon nanowire, we found that, due to the two-fold-attenuation of TPA, such a phase shift necessitates a propagation loss as low as 0.2 dB/cm. This ultralow loss is very challenging for even state-of-art fabrication technologies (which is 0.45 dB/cm [19]). A similar conclusion has been originally drawn in both [20] and a very recent work [21]. Furthermore, according to our calculations, the idea of moving from the telecommunications window to the spectral region around 2.2 μm (where the TPA vanishes) does not guarantee a larger phase shift, because the nonlinearity also decreases after reaching its maxima at a wavelength of 1.9 μm [22]. Instead, the required effective phase shift is achievable in silicon waveguides with a propagation loss of 0.45 dB/cm at a wavelength of 1.9 μm by taking advantage of the large nonlinearity and moderate TPA.

In conclusion, we investigated single- and multi-channel one-pump phase-sensitive amplification in a Hydex waveguide. We show the simple manipulation of the individual channels via adjustments of their initial phase. We find that any (linear or nonlinear) loss fundamentally limits the maximum gain in $\chi^{(3)}$-media due to a two-fold-attenuation effect. By combining an ultra-low loss and a moderate nonlinearity, Hydex can exhibit a large net gain (>10 dB) along with a significant extinction ratio (>24 dB), not achievable in other integrated Kerr media despite their higher nonlinearities. We further extend this scheme to multi-channel PSA, and our results suggest that multi-channel on-chip PSA is a promising scheme for controlling and manipulating optical channels in signal processing, and that Hydex waveguides are an attractive medium for this PSA scheme, without the need for implementing PIN junctions or any other additional complexity.

This work was supported by the Strategic and Discovery Grants Schemes (NSERC), Canada Research Chair Program, MESI PSR-SIIRI Initiative, NSERC Vanier Canada Graduate Scholarships (C.R. and P.R.), Mitacs IT06530 (Y.Z.), European Union's FP7 Programme (PIOF-GA-2013-625466, B.W.), Marie Skłodowska-Curie grant (656607, M.K.), ITMO Fellowship and Professorship Program (074-U01) and 1000 Talents Sichuan Program (R.M.).

References

1. T. Umeki, O. Tadanaga, M. Asobe, Y. Miyamoto, and H. Takenouchi, Opt. Express 22, 2473 (2014).
2. Z. Tong, C. Lundström, P. Andrekson, C. McKinstrie, Karlsson, D. Blessing, E. Tipsuwannakul, B. Puttnam, Toda, and L. Grüner-Nielsen, Nat. Photonics 5, 430 (2011).
3. P. Del'Haye, A. Schliesser, O. Arcizet, T. Wilken, R. Holzwarth, and T. J. Kippenberg, Nature 450, 1214 (2007).
4. A. Agarwal, J. M. Dailey, A. Agarwal, P. Toliver, and N.A. Peters, Phys. Rev. X 4, 041038 (2015).
5. D. Levandovsky, M. Vasilyev, and P. Kumar, Opt. Lett. 24, 984 (1999).
6. R. Neo, J. Schröder, Y. Paquot, D. Y. Choi, S. Madden, B. L. Davies, and B. J. Eggleton, Opt. Express 21, 7926 (2013).
7. Y. Zhang, J. Schröder, C. Husko, S. Lefrancois, D.Y. Choi, S. Madden, B. L. Davies, and B. J. Eggleton, J. Opt. Soc. Am. B 31, 780 (2014).
8. Y. Zhang, C. Husko, J. Schröder, S. Lefrancois, I. H. Rey, T. F. Krauss, and B. J. Eggleton, Opt. Lett. 39, 363 (2014).
9. F. Da Ros, D. Vukovic, A. Gajda, K. Dalgaard, L. Zimmermann, B. Tillack, M.Galili, K. Petermann, and C. Peucheret, Opt. Express 22, 5029 (2014).
10. H. Sun, K.-Y. Wang, and A. C. Foster, in "CLEO: QELS" (OSA, 2015), p. FW1D–3.
11. A. Martin, S. Combrie, A. Willinger, G. Eisenstein, and A. Rossi, Phys. Rev. A 94, 023817 (2016).
12. F. Da Ros, M. Pu, L. Ottaviano, H. Hu, E. Semenova, M. Galili, K. Yvind, and L. Oxenløwe, Measurements 16, 12 (2016).
13. M.A. Ettabib, K. Bottrill, F. Parmigiani, A. Kapsalis, A. Bogris, M.Brun, P. Labeye, S. Nicoletti, K. Hammani, D. Syvridis, D. J. Richardson, and P. Petropoulos, J. Lightwave Tech. 34, 3993 (2016).
14. R. Tang, P. D. Devgan, V. S. Grigoryan, P. Kumar, and M. Vasilyev, Opt. Express 16, 9046 (2008).
15. K. Bottrill, G. Hesketh, L. Jones, F. Parmigiani, D. J. Richardson, and P. Petropoulos, Opt. Express 25, 696 (2017).
16. A. Pasquazi, Y. Park, J. Azaña, F. Légaré, R. Morandotti, B. E. Little, S. T. Chu, and D. J. Moss, Opt. Express 18, 7634 (2010).
17. Y. Zhang, C. Husko, J. Schröder, and B. J. Eggleton, Opt. Lett. 39, 5329 (2014).
18. Y. Zhang, C. Husko, S. Lefrancois, I. H. Rey, T. F. Krauss, J. Schröder, and B. J. Eggleton, Opt. Express 13, 17101 (2016).
19. S. Selvaraja, P. Heyn, G. Winroth, P. Ong, G. Lepage, C. Cailler, A. Rigny, K. Bourdelle, W. Bogaerts, D. Thourhout, J. Campenhout, and P. Absil, in OFC (USA, 2014), p.Th2A.33.
20. Y. Zhang, PhD thesis, University of Sydney (2016).
21. C. J. Krückel, P. A. Andrekson, and V. T. Company, in "CLEO-Europe" (2017), p.CD-P14.
22. A. D. Bristow, N. Rotenberg, and H. M. Van Driel, App. Phys. Lett. 90, 191104 (2007).

Reference

1. T. Umeki, O. Tadanaga, M. Asobe, Y. Miyamoto, and H. Takenouchi, "First demonstration of high-order QAM signal amplification in PPLN-based phase sensitive amplifier," Opt. Express 22, 2473-2482 (2014).
2. Z. Tong, C. Lundström, P. Andrekson, C. McKinstrie, Karlsson, D. Blessing, E. Tipsuwannakul, B. Puttnam, Toda, and L. Grüner-Nielsen, "Towards ultrasensitive optical links enabled by low-noise phase-sensitive amplifiers," Nat. Photonics 5, 430-436 (2011).
3. P. Del'Haye, A. Schliesser, O. Arcizet, T. Wilken, R. Holzwarth, and T. J. Kippenberg, "Optical frequency comb generation from a monolithic microresonator,"Nautre 450, 1214-1217 (2007).
4. A. Agarwal, J. M. Dailey, A. Agarwal, P. Toliver, and N.A. Peters, "Entangled-ppair transmission improvement using distributed phase-sensitive amplification," Phys. Rev. X 4 041038 (2015).
5. D. Levandovsky, M. Vasilyev, and P. Kumar, "Amplitude squeezing of light by means of a phase-sensitive fiber parametric amplifier," Opt. Lett. 24, 984-986 (1999).
6. R. Neo, J. Schröder, Y. Paquot, D.-Y. Choi, S. Madden, B. Luther-Davies, and B. J. Eggleton, "Phase-sensitive amplification of light in a $\chi^{(3)}$ photonic chip using a dispersion engineered chalcogenide ridge waveguide," Opt. Express 21, 7926–7933 (2013).
7. Y. Zhang, J. Schröder, C. Husko, S. Lefrancois, D.Y. Choi, S. Madden, B. L. Davies, and B. J. Eggleton, "Pump-degenerate phase-sensitive amplification in chalcogenide waveguides," J. Opt. Soc. Am. B 31, 780-787 (2014).
8. Y. Zhang, C. Husko, J. Schröder, S. Lefrancois, I. H. Rey, T. F. Krauss, and B. J. Eggleton," Phase-sensitive amplification in silicon photonic crystal waveguides," Opt. Lett. 39, 363 -366 (2014).
9. F. Da Ros, D. Vukovic, A. Gajda, K. Dalgaard, L. Zimmermann, B. Tillack, M.Galili, K. Petermann, and C. Peucheret, " Phase regeneration of DPSK signals in a silicon waveguide with reverse-biased pin junction," Opt. Express 22, 5029-5036 (2014).
10. H. Sun, K.-Y. Wang, and A. C. Foster, "Pump-Degenerate Phase-Sensitive Amplification in Amorphous Si Waveguides,"in "CLEO: QELS" (OSA, 2015), p. FW1D–3.
11. A. Martin, S. Combrie, A. Willinger, G. Eisenstein, and A. Rossi, "Interplay of phase-sensitive amplification and cascaded four-wave mixing in dispersion-controlled waveguides,"Phys. Rev. A 94, 023817 (2016).
12. F. Da Ros, M. Pu, L. Ottaviano, H. Hu, E. Semenova, M. Galili, K. Yvind, and L. Oxenløwe, "Phase-sensitive four-wave mixing in AlGaAs-on-Insulator Nano-waveguides," Measurements 16, 12 (2016).
13. M.A. Ettabib, K. Bottrill, F. Parmigiani, A. Kapsalis, A. Bogris, M.Brun, P. Labeye, S. Nicoletti, K. Hammani, D. Syvridis, D. J. Richardson, and P. Petropoulos, "All-optical phase regeneration with record PSA extinction ratio in a low-birefringence silicon germanium waveguide,"J. Lightwave Tech. 34, 3993-3998 (2016).
14. R. Tang, P. D. Devgan, V. S. Grigoryan, P. Kumar, and M. Vasilyev, "In-line phase-sensitive amplification of multi-channel CW signals based on frequency nondegenerate four-wave-mixing in fiber," Opt. Express 16, 9046-9053 (2008).
15. K. Bottrill, G. Hesketh, L. Jones, F. Parmigiani, D. J. Richardson, and P. Petropoulos, "Full quadrature regeneration of QPSK signals using sequential phase sensitive amplification and parametric saturation," Opt. Express 25, 696-705 (2017).
16. A. Pasquazi, Y. Park, J. Azaña, F. Légaré, R. Morandotti, B. E. Little, S. T. Chu, and D. J. Moss, "Efficient wavelength conversion and net parametric gain via four wave mixing in a high index doped silica waveguide," Opt. Express18, 7634-7641 (2010).
17. Y. Zhang, C. Husko, J. Schröder, and B. J. Eggleton, "Pulse evolution and phase-sensitive amplification in silicon waveguides,"Opt. Lett. 39, 5329-5332 (2014).
18. Y. Zhang, C. Husko, S. Lefrancois, I. H. Rey, T. F. Krauss, J. Schröder, and B. J. Eggleton, "Non-degenerate two-photon absorption in silicon waveguides: analytical and experimental study," Opt. Express. 13, 17101-17110 (2016).
19. S. Selvaraja, P. Heyn, G. Winroth, P. Ong, G. Lepage, C. Cailler, A. Rigny, K. Bourdelle, W. Bogaerts, D. Thourhout, J. Campenhout, and P. Absil, "Highly uniform and low-loss passive silicon photonics devices using a 300mm CMOS platform, " in OFC (USA, 2014), pTh2A.33.
20. Y. Zhang, "Phase-sensitive amplification in integrated Kerr media," PhD thesis, University of Sydney (2016).
21. C. J. Krückel, P. A. Andrekson, and V. T.-Company, "Towards on chip net gain in CMOS-compatible waveguides," in "CLEO-Europe" (2017), p. CD-P14.
22. A. D. Bristow, N. Rotenberg, and H. M. Van Driel, "Two-photon absorption and Kerr coefficients of silicon for 850–2200 nm," App. Phys. Lett. 90, 191104 (2007).